Journal of Catalysis **199,** 115–122 (2001)
doi:10.1006/jcat.2000.3155, available online at http://www.idealibrary.com on IDEAL®

Hydrophobic Ti–Si Xerogels: Catalysts for the Selective Epoxidation of Olefins and Allylic Alcohols

Yi Deng and Wilhelm F. Maier[1]

Max-Planck-Institut für Kohlenforschung, Kaiser-Wilhelm-Platz 1, D-45470 Mülheim an der Ruhr, Germany

Received September 20, 2000; revised December 8, 2000; accepted December 15, 2000

Hydrophobic amorphous mixed oxides AM-Ti$_3$^{Me}Si$_{40}$Si were prepared in the absence of modifiers as true xerogels with a narrow mesopore distribution around 3 nm. These materials selectively catalyze the quantitative conversion of olefins and allyl alcohols with an excess of oxidizing agent (TBHP). Regio- and chemoselectivity are comparable to literature data, most commonly obtained with hydrophilic aerogel catalysts and large excesses of olefin. © 2001 Academic Press

INTRODUCTION

The direct epoxidation of olefins on Ti-containing porous silicon dioxides and zeolites has received considerable attention during the last few years. Titanium-substituted silicalite-1 (TS-1) is a good catalyst for the epoxidation of small olefins with hydrogen peroxide. The success of TS-1 as an oxidation catalyst spurred the synthesis of an increasing variety of related zeolite-type catalysts, such as Ti–β, TS-2, Ti–ITQ-2, or Ti–ZSM-12 (1). Although with increasing pore size these materials can also oxidize larger alkenes, there are still limitations of molecular size and only moderate activity has been reported.

A very promising class of catalyst materials is the sol-gel-derived aerogels, amorphous Ti–Si mixed oxides with a relatively broad distribution of mesopores (9 nm), prepared under supercritical conditions. These materials show chemo- and diastereoselective behavior in the epoxidation of a wide variety of alkenes and allylic alcohols (2). The effect of organic modification of the catalyst on epoxidation behavior has been studied by varying the amounts of nonhydrolyzable methyl groups (copolycondensation of tetraethoxysilane and methyltriethoxysilane (MTES)) (2). Although the overall effects were not drastic, a significant improvement of epoxidation activity was found for the material made from 10 mol% MTES. In the catalyst preparation prehydrolysis of MTES was carried out in order to adjust for the relative rate of hydrolysis of the two alkoxides. Although this procedure is standard in the literature, it should result in the formation of methyl-rich domains (block copolymers) rather than in a homogeneous distribution of covalent methyl groups throughout the materials. Replacing these nonhydrolyzable methyl groups with fictionalized organic groups resulted, in some examples, in additional improvements of the catalytic activity of these aerogels. When 3-acetoxypropyltrimethoxysilane was used in the aerogel preparation, significant rate and selectivity increases were reported for the epoxidation of cyclohexene and cyclohexenol (3). By introducing the *N*,*N*-dimethyl-3-aminopropyl group an epoxidation selectivity of 93% at 100% TBHP conversion was observed. (4). Clearly, the presence of organic groups can improve the activity and selectivity of these catalysts, but so far these new effects are empirically found and are not understood in detail.

The discovery of Ti-substituted molecular sieve (TS-1) allowed the use of environmentally friendly H_2O_2 as the oxidant for selective oxidation (5). The special activity of TS-1 is due to the tetrahedrally coordinated Ti in the framework, its hydrophobic nature, and Lewis-acidic Ti^{IV-} sites (6). Due to its small pores TS-1 is often claimed not to be active in the oxidation of bulky molecules. To overcome this limitation large-pore titanium-containing zeolites were synthesized, Ti–β (7–10), Ti–HMS (11), and Ti–MCM-41 (12, 13), but their performances were not comparable to that of TS-1 (14). Selective oxidation of unsaturated alcohols has been reported by Sheldon *et al.* with TS-1 and H_2O_2 (15). With TS-1 and urea peroxide or Ti–β zeolites and H_2O_2, diastereoselective oxidation of allylic alcohols has been reported. In comparison with homogeneous Ti catalysts significant selectivity differences are observed. However, despite the much smaller pores of TS-1 little difference in relative activity or selectivity compared to Ti–β is reported, indicating a lack of pore size effects. The large amount of catalyst used and the relatively long reaction times of 12–24 h seem to be the major drawbacks (16).

Another group of materials useful for double bond epoxidations is the Ti-containing MCM-type materials. These materials have a very narrow distribution of mesopores and as such are an interesting alternative to the Ti–Si aerogels,

---

[1] To whom correspondence should be addressed.

0021-9517/01 $35.00

which have a much broader pore size distribution. With a MCM-41 catalyst containing Ti in the framework, a lower total activity was reported for epoxidation reactions relative to TS-1 or Ti–β zeolites (17). Higher selectivity and activity for the epoxidation of cyclohexene was reported for a MCM-41 catalyst grafted with the Ti–Cp_2Cl_2 complex as the active site (18). The same complex had already been used in the preparation of a sol–gel-derived silica-based catalyst, active and selective for epoxidations of nonactivated olefins (19).

In the past we have demonstrated that amorphous microporous mixed oxides (AMM) with a narrow pore size distribution (comparable to that of zeolites) can be prepared by simple sol–gel procedures. A variety of Ti–Si mixed oxides (AMM-Ti_xSi) were prepared from titanium tetraisopropoxide (TIPOT) and tetraethoxysilane (TEOS) under acidic sol–gel conditions. Since these materials are prepared in solution and dried in the open atmosphere, they can be classified as xerogels. Ultra violet diffusive reflectance (UV-DRS) studies showed that Ti is homogeneously distributed in these materials (20). This has been confirmed by EXAFS studies as well as by high-resolution transmission electron microscopy (HRTEM) with selected area energy dispersive X-ray analysis (EDX) (21). These materials are active and selective for alkene epoxidation with TBHP (22), although a 4 : 1 excess of alkene over TBHP had to be used. A drastic decrease in epoxidation turnover frequency was observed with increasing molecule size (from 1-hexene to 1-pentadecene), confirming a significant pore size effect (shape selectivity) comparable to that of TS-1 (21, 23). However, in all these reactions, excess olefin was used and, still, maximum TBHP conversion was limited to about 40%. By copolycondensation of TEOS and TIPOT with MTES nonhydrolyzable methyl groups were introduced into the amorphous framework, resulting in a dramatically improved catalytic performance. Not only did the total conversion increase from about 40 to 100%, but even hydrogen peroxide could be used as oxidizing reagent (24). It was shown that with increasing Me content the materials became increasingly hydrophobic. With pulse field gradient NMR it has been shown that this increased hydrophobicity does not affect the diffusion of unpolar hydrocarbons in the micropores, but drastically increases the mobility of water and polar molecules (25). Apparently, polar molecules, such as products, reagents, or impurities, clog micropores with hydrophilic surfaces. It has been shown that the activity and selectivity of these amorphous catalysts are comparable to that of the crystalline TS-1 in various selective oxidation reactions (24). Although several problems of selective oxidation could be addressed with these AMM materials, the narrow pore size of these microporous materials still represented a major limitation.

We report here the preparation of hydrophobic *mesoporous* amorphous mixed oxides (AM) in the absence of modifiers or templates (true xerogels) and their performance relative to their *microporous* counterpart (AMM) as selective oxidation catalysts under liquid phase reaction conditions.

EXPERIMENTAL

All solvents and reactants were dried carefully prior to the reactions.

Catalyst Preparations

Microporous catalyst. For the preparation of AMM-$Ti_3{}^{Me}Si_{40}Si_{57}$: 40 mmol MTES and 57 mmol TEOS were placed in a 100-ml PP beaker equipped with a magnetic stirring bar and mixed with 3 mmol titanium propoxide. After agitation for 15 min this solution was diluted with 300 mmol ethanol. Subsequently 4.38 ml HCl (8 mol/liter) was added dropwise to the well-stirred solution, which turned from colorless to yellow.

Drying procedure. The clear solution in the beaker was densely covered with polyethene foil and stirred for another 24 h. The polyethene foil was taken off to allow evaporation of the volatiles. The gelation occurred within 1–2 days. After 5 days the sample was heated from room temperature up to 338 K with 0.1 K/min and kept at this temperature for 100 min. Then, the temperature was allowed to rise to 523 K at the rate of 0.1 K/min for 5 h. Finally the samples were cooled down to room temperature at the a rate of 2 K/min. The glass was then crushed with a mortar and milled in a ball mill for 20 min. The materials have been characterized previously (24). For simplification, this *microporous* catalyst hereafter is identified as AMM-Ti3.

Mesoporous catalyst. The preparation of AM-Ti_3 ${}^{Me}Si_{40}Si_{57}$ followed the same procedure as the microporous catalyst, except for the drying process, which was modified.

Drying procedure. Thereafter the clear solution in the beaker was densely covered with polyethene foil and stirred for another 24 h. Then the solution in the beaker was placed in the hood for 4 weeks. Then the foil was punctured with about 10 holes to allow for slow evaporation of the solvent and allowed to stand for another 3 months. Thereafter the sample was heated from room temperature up to 338 K with 0.1 K/min and kept at this temperature for 100 min. Then, the temperature was allowed to increase to 523 K at the rate of 0.1 K/min for 5 h. Finally the samples were cooled down to room temperature at the rate 2 K/min. The glass was then crushed in a ball mill for 20 min. For simplification, this *mesoporous* catalyst hereafter is identified by the abbreviation AM-Ti3.

Characterization

Physisorption. Argon physisorption measurements were collected on an Omnisorb 360 (Coulter). The samples were outgassed prior to measurement at 523 K and 10^{-4} mbar for 12 h. Adsorption isotherms were recorded using a static volumetric technique with a starting pressure of 5 Torr that was increased by a factor of 1.05 for every dosage step. Argon was adsorbed at a temperature of 87.4 K (Ar_{lq}). The pore size distributions were calculated for the microporous samples using the Horvath–Kawazoe model, while, for the mesoporous materials the Barrett–Joyner–Halenda theory was applied (26). The absence or presence of micropores was identified by the absence or presence of a point of inflection at the low pressure region of the Ar-adsorption isotherm (27). For the surface area determination the BET variation of Dubinin was applied.

X-ray diffraction. X-ray powder diffraction (XRD) patterns were measured using the Debye–Sherrer technique on a Stoe Stadi 2/PL diffractometer using Cu$K\alpha$ radiation in the range of $2\theta = 10$–90°. The detector used was an area detector PSD1. All powered gels were studied at room temperature after calcination.

Electron microscopy. The glasses were examined with HRTEM on a Hitachi HF 2000 instrument combined with EDX. The amorphous nature of the materials was examined by electron diffraction (magnification, 200 K; camera length, 0.2 m) and high-resolution imaging. The samples were crushed in an agate mortar in a methanol suspension and transferred to a Holey carbon grid (copper, 3 mm in diameter).

Infrared spectroscopy. Fourier transform infrared transmission spectra (FTIR) of the catalysts were collected with a Bruker IFS 48 Fourier transform spectrometer with a spectral resolution of 2 cm^{-1} at 200 scans and the experimental data were displayed using the Kubelka–Munk function (dry KBr as background). For DRIFTS measurements the catalyst was dried *in situ* at 400°C for 12 h in a flow of dry argon using a reaction chamber (Harrick HVC) in combination with a diffuse reflectance unit (Harrick DRA-XX). This drying procedure is essential to remove Si–OH bands around 960 cm^{-1}, which otherwise obscure the Si–O–Ti band at the same spectral region (21).

UV spectroscopy. UV spectroscopy was carried out on a Varian Cary 05 UV-VIS-NIR spectrometer in DRS. The spectra were recorded either under ambient conditions or under dry conditions using a special quartz cell, which allowed heat treatment (2 h at 673 K in a flow of argon) and measurement in a moisture-free atmosphere. The Kubelka–Munk function was used to display the data (28).

Catalytic Testing

The catalysts were heated to a temperature of 250°C for 3 h in a constant stream of argon to remove all traces of water before use. All conversions given are conversions of starting alkenes and selectivities given relate to the desired product and are based on this conversion.

Epoxidation of olefins. Olefin (5 mmol) and 10 mmol of TBHP (solution in *i*-octane, 4 mol TBHP/liter; ratio of olefin:TBHP, 1 : 2) were mixed in the presence of 50 mg of catalyst in a glass microreactor equipped with a magnetic stirrer and heated to 80°C. Conversion was monitored by taking samples and analyzing them by gas chromatography (GC).

Epoxidation of allylic alcohols. Allylic alcohol (8 mmol) and 8 mmol of TBHP (4 M TBHP in *i*-octane; ratio of olefin:TBHP, 1 : 1) were mixed in the presence of 50 mg of catalyst in a glass microreactor equipped with a magnetic stirrer and heated to 80°C. The conversion was monitored by GC. The products were identified by gas chromatography/mass spectroscopy, by GC, or by comparison with authentic samples. At the analysis of the products in the epoxidation of the secondary allylic alcohols preparative gas chromatography was used to obtain the pure products and their structures were then identified by ^{1}H-NMR and ^{13}C-NMR.

RESULTS AND DISCUSSION

Catalyst Preparation and Characterization

Both catalysts were prepared by modified sol–gel procedures. To avoid domain formation the Ti content was kept at 3% (21). To adjust the relative rate of hydrolysis of MTES relative to TEOS prehydrolysis of MTES is commonly applied before the TEOS addition. Although this is common practice in the literature, we chose not to use prehydrolysis for the simple reason that prehydrolysis must result in the formation of MTES domains. This in turn must result in the formation of hydrophobic islands, which in turn will promote the formation of hydrophilic islands on the silica formed from TEOS, which is usually only added after prehydrolysis. In other words, we assume that prehydrolysis will result in the formation of block copolymers rather than true copolymers as desired by us. Our interest is in preparing a material as homogeneous in elemental distribution and functionality as possible. Therefore, reaction conditions were optimized to provide a clear homogeneous glass during the whole sol–gel transformation, in which both components, MTES and TEOS, were copolymerized simultaneously. Since the microporous AMM material has been characterized before (24), mainly the new characterization data of the mesoporous material are reported here.

Physisorption. The methods applied rely on previous studies of the pore architecture and size of these amorphous mixed oxides. We have shown that micropore diameters can only be identified reliably by the presence of a point of inflection in the low pressure region ($p/p_0 < 10^{-1}$) of high-resolution adsorption isotherms obtained with Ar at the temperature of Ar_{lq}. The adsorption isotherms are shown in Fig. 1 and surface areas and pore volumes, as deduced

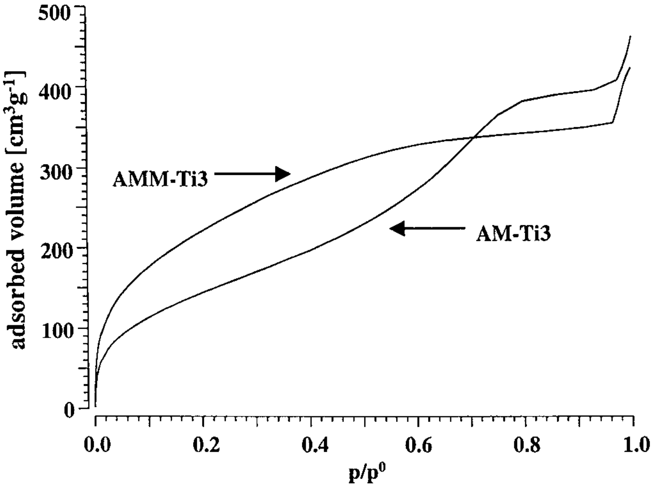

FIG. 1. Argon adsorption isotherms of AMM-Ti$_3$ and AM-Ti$_3$.

from the adsorption isotherms, are listed in Table 1. The maximum pore size of AM-Ti3 is 3.0 nm while that of AMM-Ti3, which has the same composition as AM-Ti3, is 0.70 nm. The surface area of AM-Ti3 is lower than that of AMM-Ti3.

X-ray diffraction. Both materials are X-ray amorphous; the spectra are very similar. The XRD spectrum of the AM-$Ti_3{}^{Me}Si_{40}Si$ is shown in Fig. 2.

Electron microscopy (HRTEM/EDX). HRTEM and EDX were used to investigate the textural properties of the catalysts at atomic resolution. Neither electron diffraction patterns, typical of crystalline samples, nor crystalline lattice fringes could be detected in the catalysts. A typical micrograph of the AM-catalysts is shown in Fig. 3. The elemental compositions obtained from selected area EDX analyses confirmed the expected compositions from the synthesis. No evidence of the formation of domains or enrichments has been obtained, indicating that the Ti centres are on isomorphic positions in the amorphous silica lattice.

FTIR spectroscopy. The DRIFT spectrum of AM-Ti3 is given in Fig. 4. Surface SiOH bands, usually obscuring the 900–1000 cm^{-1} region, have been removed through the temperature treatment at 673 K prior to the measurement. The band at 960 cm^{-1} is thus characteristic of titanium silicate molecular sieves (29). This band at 960 cm^{-1} is considered evidence for the isomorphous substitution of Si by Ti (Si–O–Ti vibration) in amorphous mixed oxides (21, 30, 31). The band at 1280 cm^{-1} is assigned to the Si–C vibration of the methyl group (2, 24).

TABLE 1

Physisorption Results

Catalyst	S_{BET} (m^2/g)	Pore volume (cm^3/g)	Pore size[a] (nm)
AMM-Ti3	734	0.44	0.71
AM-Ti3	479	0.58	3.1

[a] Maximum pore size distribution.

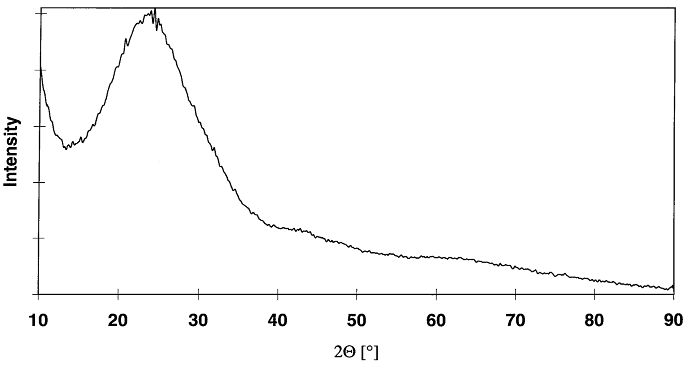

FIG. 2. XRD pattern of AM-Ti3.

UV spectroscopy (DRS). The adsorption band at 210 nm for TS-1 is attributed to isolated Ti(IV) framework sites in tetrahedral coordination (32, 33). The band at 220 nm, which is also present in TS-1 and Ti–Beta, has been assigned to the ligand-to-metal charge transfer (CT) involving isolated Ti atoms in octahedral coordination, in which two water molecules take part (17). Peaks between 300 and 350 nm indicate the presence of anatas (34, 35).

The catalysts obtained directly after calcination showed the presence of a band at 210 nm. After a long period in moist atmosphere the band shifted to 220 nm. After heating under argon the band at 210 nm could be recovered, indicating that its disappearance can be associated with the reversible adsorption of water. Since the catalyst activity is highest after such a heating process, it is assumed that the activity decrease is directly associated with water adsorption to the Ti sites. No peaks between 300 and 350 nm were detected (Fig. 5).

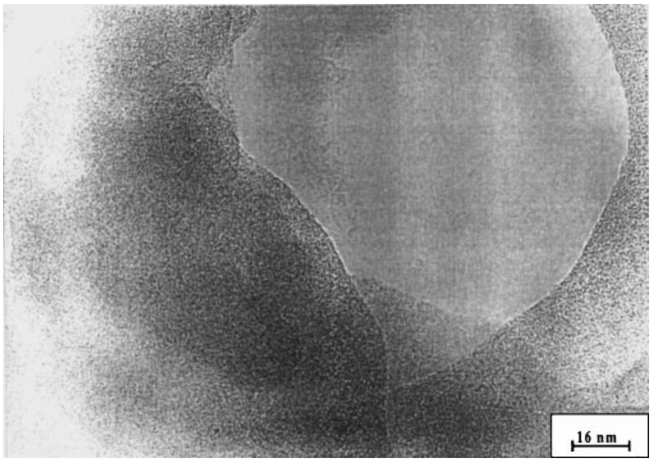

FIG. 3. High-resolution transmission electron micrograph of AM-Ti3.

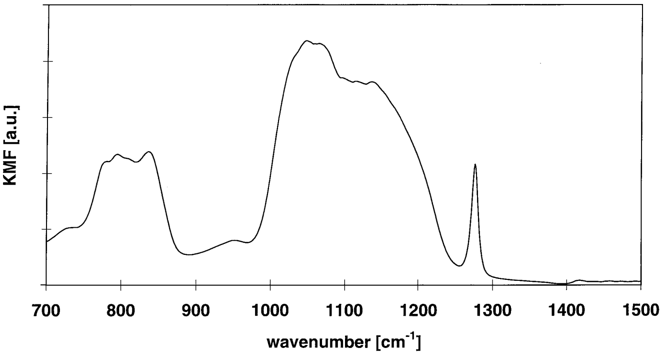

FIG. 4. DRIFT spectrum of AM-Ti3.

Selective Oxidations

Influence of olefin : hydroperoxide molar ratio. In the literature commonly high olefin : hydroperoxide molar ratios are applied to achieve the desired high epoxide selectivities. Due to competing decomposition of hydroperoxide, lower olefin : hydroperoxide ratios often lead to lower selectivities with increasing olefin conversion (36, 37). Different ratios were used to test their influence on the selectivities to epoxide (Table 2). With our catalysts high selectivities were obtained even at the low olefin : hydroperoxide ratio of 1 : 2), indicating a remarkable selectivity of the catalysts toward double bond oxidation.

Activity comparison with AMM-Ti3. Due to more efficient molecular transport through the mesopores we expected to see a higher rate of reaction on the AM-catalyst. When the activity of the mesoporous AM-Ti3 for the epoxidation of 1-octene was compared with that of the microporous AMM-Ti3 (Fig. 6), it was surprising to see no difference in selectivity and a slightly higher reaction rate on the microporous catalysts. The same relative behavior was observed for the oxidation of cyclohexane (37). Due to the lack of additional information, we can only speculate that the size of the molecules studied is still small enough to be transported effectively through the 0.8-nm micropores of the AMM materials.

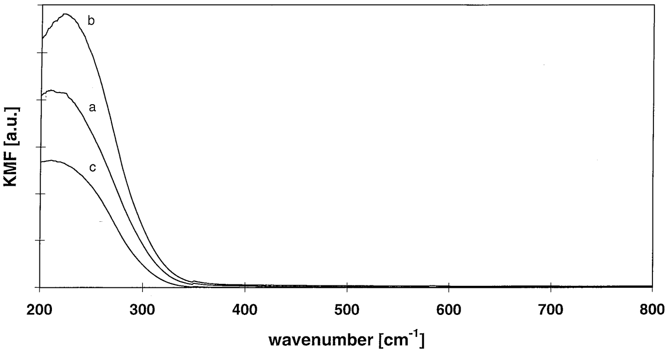

FIG. 5. UV-DRS spectra of AM-Ti3 (a) Directly after calcination, (b) under ambient conditions after several months, and (c) after drying under argon at 250°C for 2 h.

TABLE 2

Effect of 1-Octene/TBHP-Ratio on Epoxidation of 1-Octene

1-Octene : TBHP	Conversion of 1-octene (%)	Selectivity to epoxide (%)
5 : 1	13.7	100
1 : 1	30.9	99.0
1 : 2	32.3	99.1

Note. Reaction temperature, 80°C; total volume, 3.3 ml; reaction time, 5 h.

Heterogeneity test. Homogeneous Ti–isopropoxide is a good epoxidation catalyst. To investigate the heterogeneous nature of the reactions, the solid AM-catalyst was filtered off with a 0.02-μm syringe filter at the reaction temperature of 80°C after 1.5 h. It has been shown previously that filtration at lower temperatures results in readsorption of dissolved homogeneous species on the solid surface, thus falsifying the results (38). Reference experiments were performed under identical reaction conditions. The test reactions for epoxidation of cyclooctene and 3-methyl-2-butene-1-ol are shown in Figs. 7 and 8, respectively. After filtration conversion essentially stopped, the very slow increase detected is attributed to nanoparticles not removable by filtration. The Ti content in the mother liquor did not exceed the detection limit. The conversion in the reference experiments continued. The epoxidations catalyzed by AM-Ti3 are truly heterogeneous.

Epoxidation of the different olefins. Table 3 summarizes the results of alkene oxidations with the mesoporous AM-Ti3. In contrast to the state of the art with alternative aerogel catalysts and Ti–silicalites, we can now use equimolar amounts or even an excess of TBHP in order to drive alkene conversion to completion. For the first time, we report here total conversion of alkenes with epoxide selectivities larger than 90%. The best result was achieved with 1-octene, which

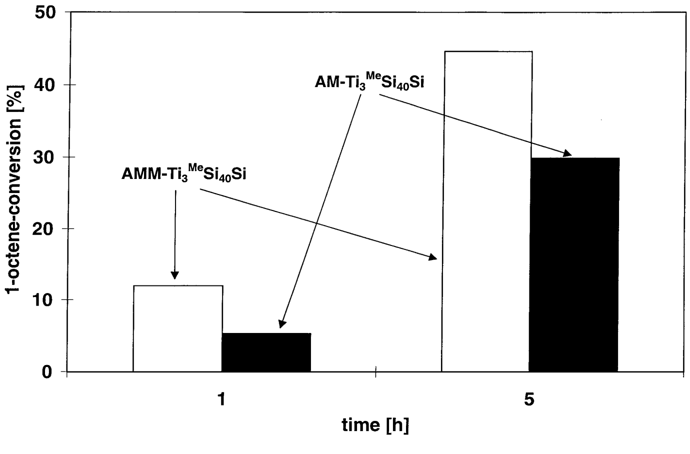

FIG. 6. Effect of pore size on the catalytic activity of the catalysts indicated for the epoxidation of 1-octene with TBHP.

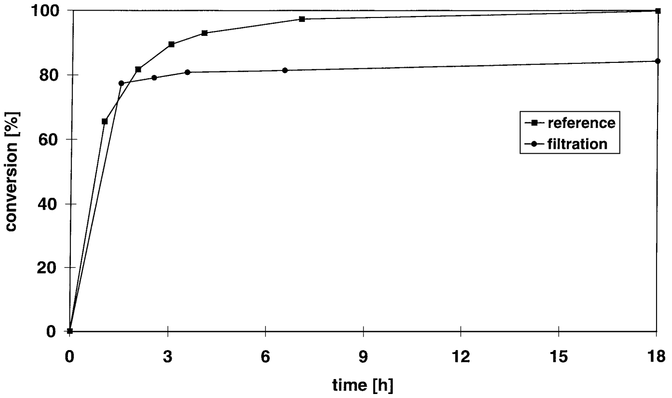

FIG. 7. Effect of the removal of the AM-Ti3 catalyst after 1.5 h on the epoxidation of cyclooctene.

has been quantitatively converted to the epoxide with a selectivity of almost 99% (uncorrected GC data).

The reactivity of the α-olefins decreases with increasing chain length, 1-hexene > 1-octene, and increases with increasing electron density on the double bond, cyclooctene, *cis*-2-hexene, cyclohexene > 1-methyl-1-cyclohexene > *trans*-2-hexene > 1-hexene. Relative reactivities depend mainly on the nucleophilicity of the double bond, which parallels the characteristics of homogeneously catalyzed epoxidations (36, 40). However, the much slower reactions of cyclododecene and 1-octene must be attributed to molecular size or diffusion effects. The retention of stereochemical configuration has been observed: *cis*-2-hexene gives exclusively the *cis*-epoxide, and *trans*-2-hexene gives exclusively the *trans*-epoxide. The high selectivities observed with a wide range of olefins and the stereospecificity of the reaction are consistent only with a heterolytic mechanism. With TS-1 1-hexene reacts much faster than cyclohexene. This has been attributed to steric factors, where cyclohexene is already hindered in entering the small pores of the silicalite (41). With our AM material cyclohexene reacts much faster than 1-hexene, which is also observed with the Ti–Si aerogels. All the olefins can be almost quantitatively oxidized to epoxides.

TABLE 3

Alkene Oxidations with TBHP and AM-Ti3

Reactant	Time [h]	Product	Alkene conversion [epoxide selectivity] [%]	TOF[*] $[\mathrm{h}^{-1}]$
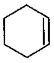	16	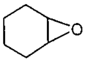	100 [90.8]	79.1[a]
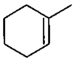	21	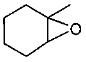	100 [92.8]	100.2
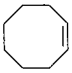	8	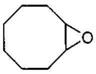	97.1 [99.5]	102.5
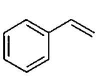	154	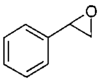	98.0 [92.6]	49.5
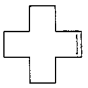 (cis- und trans-)	485	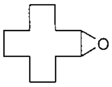 (cis- und trans-)	90.0 [89.9]	38.6
	25	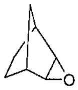	97.6 [94.3]	54.7
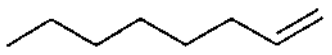	168	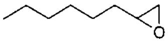	100 [98.9]	15.8
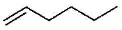	72	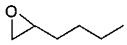	89.5 [92.6]	21.7
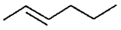	48	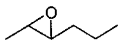	94.5 [98.0]	48.1
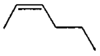	8	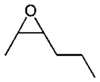	96.4 [98.7]	105.3

[*] Reaction time, 1 h.
[a] Using 5 M TBHP in nonane.

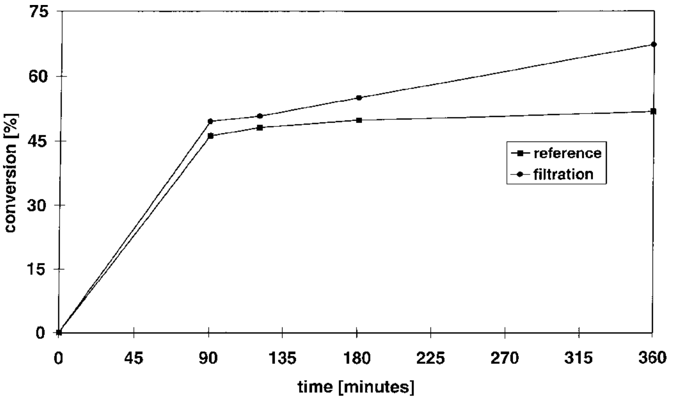

FIG. 8. Effect of the removal of the AM-Ti3 catalyst after 1.5 h on the epoxidation of 3-methyl-2-butene-1-ol.

Epoxidation of allylic alcohols. Epoxidation of primary allylic alcohols and homoallylic alcohols has been tested; the results are listed in Table 4. Double bond oxidation to the epoxides dominates in all cases. Conversions are high, but not as quantitative as with the alkenes. The rate of reaction is no function of chain length or double bond reactivity, as documented with the rapid conversion of the geraniol. The epoxidation selectivity of 3-methyl-2-butene-1-ol is with 83% the lowest. The double bond near the hydroxyl group was oxidized preferentially in the epoxidation of geraniol. The selectivity ratio of two double bonds is 4.5 : 1. This preference illustrates that a hydroxyl group is able to regioselectively deliver the oxidant to the less electron-rich double bond of a diene (36, 42, 43). With microporous AMM-Ti3 the oxidation of geraniol proceeds at the same rate as on AM-Ti3, but the selectivity is slightly higher, indicative of an onset of shape selectivity.

TABLE 4

Oxidation of Primary Allylic and Homoallylic Alcohols with TBHP and AM-Ti3

Reactant	Time [h]	Product	Alkene conversion [epoxide selectivity] [%]
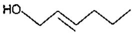	166	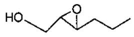	79 [85]
	166	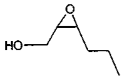	87 [91]
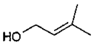	6	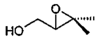	78 [83]
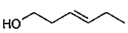	120	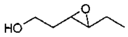	82 [92]
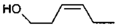	55		84 [95]
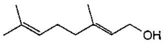	5	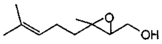	63 [63][1] 69 [75]*[2]

[1] Selectivity to epoxide at the end side double bond is 14%.
[2] Selectivity to epoxide at the end side double bond is 8%.
* With AMM-Ti3.

Diastereoselectivity is documented in Table 5 with the epoxidation of secondary allylic alcohols. Threoepoxide formation is clearly preferred, which has also been observed with Ti aerogels (44) as well as with Ti-catalyzed homogeneous epoxidations (45). The AM-catalyst is more active for the epoxidation of *trans*-3-pentene-2-ol and cyclohexenol, which both possess an internal C=C double bond, relative to the alcohols with terminal double bonds. Its higher reactivity may be due to the higher electron density resulting from the electron-releasing effect of the alkyl group (44). Cyclohexenol can be epoxidized preferentially to *cis*-epoxide. Temperature has no influence on diastereoselectivity, which contrasts with the results with homogeneous catalyst that asymmetric synthesis increases when the reaction temperature is lowered (46). Pore size has little influence on diastereoselectivity, as shown in the epoxidation of cyclohexen-3-ol with microporous AMM-Ti3 and mesoporous AM-Ti3. Again, in contrast to initial expectations, the reaction rate is slightly lower on the mesoporous relative to the microporous catalyst.

TABLE 5

Epoxidation of Secondary Allylic Alcohols with TBHP and AM-Ti3

Reactant [%][a]	Time [h]	Product	Threo/ Erythro [%]	Alkene conversion [epoxide selectivity]
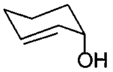	2		78/22[b]	40 [92]
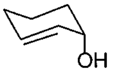	2		89/11	58 [91][c]
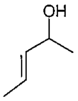	74	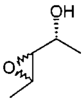	62/38	33 [93][d]
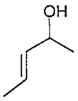	1 26	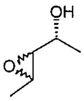	67/33 67/33	39 [96] 78 [95]
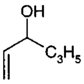	48	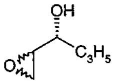	56/44	50 [94]
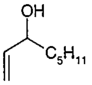	44	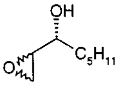	57/43	57 [91]

[a] Temperature, 353 K.
[b] *cis/trans.*
[c] Catalyzed by AMM-Ti3.
[d] Temperature, 313 K.

TABLE 6

Effect of Alcohol Function on the Epoxidation of Olefins

Reactant	Time [h]	Product	Alkene conversion [epoxide selectivity] [%]	TOF* [h^{-1}]
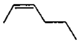	1	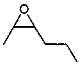	48.8 [99.1]	112.8
	1	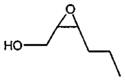	24.5 [90.5]	56.6

* Reaction time, 1 h.

In homogeneous metal-catalyzed epoxidations, introducing an allylic hydroxyl group can result in a dramatic overall rate enhancement (36, 42, 43). The opposite is true for the heterogeneously catalyzed epoxidation with the AM-catalyst (see Table 6). Epoxidation of *cis*-2-hexene proceeds twice as fast as that of *trans*-2-hexen-1-ol, confirming the trend already observed with the aerogel-catalyzed epoxidation (44). This reduction of rate is attributed to mass transport effects, i.e., slower rates of diffusion of the more polar and larger alcohols in the catalyst pores.

CONCLUSION

Two hydrophobic amorphous Ti–Si mixed oxides of identical chemical composition, one mesoporous and one microporous, have been prepared by copolycondensation of MTES, TEOS, and titanium propoxide in a one-step procedure by an acid-catalyzed sol–gel process in the open air in the absence of any modifier. Both materials have been obtained as xerogels (no supercritical conditions). The materials have narrow pore size distributions and the Ti is homogeneously distributed in the amorphous silica lattice. The materials are very active and selective catalysts for the epoxidation of bulky olefins and allylic alcohols in the liquid phase. There is little difference in the activity and selectivity of these two materials. It is unusual that the reactions can be carried out with excess oxidizing agents, which allows quantitative conversion of the olefin at selectivities exceeding 90%. The lack of secondary reactions observed is attributed to the hydrophobic nature of the catalysts, the low Ti content, and/or the lack of acidic sites.

ACKNOWLEDGMENTS

Y. Deng thanks the Konrad-Adenauer-Stiftung for a fellowship. We thank Dr. R. Mynott for the NMR analyses, E. Hübinger and S. Ruthe for GC analyses, and D. Stoffels and W. Reissig for prep-GC analyses. We thank C. Lettmann for TEM measurements and H. Bretinger for the sorption analyses.

REFERENCES

1. Sheldon, R. A., *J. Mol. Catal. A* **107**, 75 (1996).
2. Müller, D. C., Maciejewski, M., Mallat, T., and Baiker, A., *J. Catal.* **184**, 280 (1999).
3. Müller, C. A., Schneider, M., Gisler, A., Mallat, T., and Baiker, A., *Catal. Lett.* **64**, 9 (2000).
4. Müller, C. A., Schneider, M., Mallat, T., and Baiker, A., *J. Catal.* **189**, 221 (2000).
5. Taramasso, M., Perego, G., and Natari, B., U.S. Patent 4,410,501, 1983.
6. Bellussi, G., and Rigutto, M. S., *Stud. Surf. Sci. Catal.* **85**, 177 (1994).
7. Jappar, N., Xia, Q. H., and Tatsumi, T., *J. Catal.* **180**, 132 (1998).
8. Blasco, T., Cablor, M. A., Corma, A., Esteve, P., Guil, J. M., Martínez, A., Perdigón-Melón, J. A., and Valencia, S., *J. Phys. Chem. B* **102**, 75 (1998).
9. Cablor, M. A., Corma, A., and Perez-Pariente, J., *Zeolites* **13**, 82 (1993).
10. Reddy, J. S., and Sayari, A., *J. Chem. Soc. Chem. Commun.* 23 (1995).
11. Tanev, P. T., Chibwe, M., and Pinnavaia, T. J., *Nature* **368**, 321 (1994).
12. Corma, A., Camblor, M. T., Esteve, P., Martinez, A., and Perez-Pariente, J., *J. Catal.* **145**, 151 (1994).
13. Corma, A., Navarro, M. T., and Perez-Pariente, J., *J. Chem. Soc. Chem. Commun.* 147 (1994).
14. Tasumi, T., Yako, M., Nakamura, M., Yuhara, Y., and Tominaga, H., *J. Mol. Catal.* **78**, L41 (1993).
15. Sheldon, R. A., Arends, I. W. C. E., and Lempers, H. E. B., *Catal. Today* **41**, 387 (1998).
16. Adam, W., Corma, A., Martínez, A., Mitchell, C. M., Reddy, T. I., Renz, M., and Smerz, A. K., *J. Mol. Catal. A* **117**, 357 (1997).
17. Blasco, T., Corma, A., Navarro, M. T., and Pérez Pariente, J., *J. Catal.* **156**, 65 (1995).
18. Maschmeyer, T., Rey, F., Sankar, G., and Thomas, J. M., *Nature* **378**, 159 (1995).
19. Thorimbert, S., Klein, S., and Maier, W. F., *Tetrahedron* **51**, 3787 (1995).
20. Klein, S., Maier, W. F., Weckhuysen, B. M., Martens, J. A., and Jacobs, P. A., *J. Catal.* **163**, 489 (1996).
21. Klein, S., Thorimbert, S., and Maier, W. F., *J. Catal.* **163**, 476 (1996).
22. Klein, S., Martens, J., Parton, R., Vercruysse, K., Jacobs, P. A., and Maier, W. F., *Catal. Lett.* **38**, 209 (1996).
23. Corma, A., Esteve, P., Martínez, A., and Valencia, S., *J. Catal.* **152**, 18 (1995).
24. Klein, S., and Maier, W. F., *Angew. Chem.* **108**, 2376 (1996); *Angew. Chem. Int. Ed. Eng.* **35**, 2230 (1996).
25. Krause, C., Klein, S., Kärger, J., and Maier, W. F., *Adv. Mater.* **8**, 912 (1996).
26. Seifert, J., and Emig, G., *Chem. Ing. Tech.* **59**, 475 (1987).
27. Storck, S., Bretinger, H., Maier, W. F., *Appl. Catal. A: Gen.* **174**, 137 (1998).
28. Kubelka, P., and Munk, F., *Z. Tech. Phys.* **12**, 593 (1931).
29. Kumar, S. B., Mirajkar, S. P., Pais, G. C. G., Kumar, P., and Kumar, R., *J. Catal.* **156**, 163 (1995).
30. Davis, R. J., and Liu, Z., *Chem. Mater.* **9**, 2311 (1997).
31. Kosuge, K., and Singh, P. S., *J. Phys. Chem. B* **103**, 3563 (1999).
32. Thangaraj, A., Kumar, R., Mirajkar, S. P., and Ratnasamy, P., *J. Catal.* **130**, 1 (1990).
33. Zhang, W., Froba, M., Wang, J., Tanev, P. T., Wong, J., and Pinnavaia, T. J., *J. Am. Chem. Soc.* **118**, 9164 (1996).
34. Dartt, C. B., Khouw, C. B., Li, H. X., and Davis, M. E., *Microporous Mater.* **2**, 425 (1994).
35. Khouw, C. B., Dartt, C. B., Labinger, J. A., and Davis, M. E., *J. Catal.* **149**, 195 (1994).
36. Sheldon, R. A., *J. Mol. Catal.* **7**, 107 (1980).
37. Hutter, R., Mallat, T., and Baiker, A., *J. Catal.* **157**, 665 (1995).
38. Hunnius, M., Ph.D. thesis, University of GH Essen, 1998.
39. Vanoppen D. L., Devos, D. E., Genet, M. J., Rouxhet, P. G., and Jacobs, P. A., *Angew. Chem.* **107**, 637 (1995).
40. Sobczak, J., and Ziolkowski, J. J., *J. Mol. Catal.* **13**, 11 (1981).
41. Romano, U., Esposito, A., Maspero, F., Neri, C., and Clerici, M. G., *Stud. Surf. Sci. Catal.* **55**, 33 (1990).
42. Hoveyda, A. H., Evans, D. A., and Fu, G. C., *Chem. Rev.* **93**, 1307 (1993).
43. Sheldon, R. A., and Kochi, J. K., “Metal-Catalyzed Oxidations of Organic Compounds.” Academic Press, New York, 1981.
44. Dusi, M., Mallat, T., and Baiker, A., *J. Mol. Catal. A* **138**, 15 (1999).
45. Martin, V. S., Woodard, S. S., Katsuki, T., Yamada, Y., Ikeda, M., and Sharpless, K. B., *J. Am. Chem. Soc.* **103**, 6237 (1981).
46. Mihelich, E. D., *Tetrahedron Lett.* **49**, 4729 (1979).